

Toner Usage Prediction for Laser Electrophotographic Printers

Mengqi Gao[1], Yanling Ju[1], Terry Nelson[2], Theresa Prenn[2], and Jan Allebach[1]

[1]School of Electrical and Computer Engineering, Purdue University, West Lafayette, IN
[2]Hewlett-Packard Company, Boise, ID

***Abstract*—In recent years, laser electro-photographic (EP) printers are commonly used in both industry and households. From an economic perspective, it is of great significance to accurately estimate toner usage in order to get a full utilization of each cartridge. A revised two-stage strategy is developed based on the 'black box 'model which demonstrate that the toner deposition in the area occupied by each printer-addressable pixel is strongly influenced by the values of the neighboring pixels.**

For the first stage, the pixel-by-pixel absorptance is predicted from the digital page image that is sent to the laser engine, and trained from a set of printed and scanned pages. Then, during stage two, the overall toner usage for input digital page can be estimated by using a weighted sum method that adds up the weight of every individual pixel of the whole page. The weights of pixels are trained by using the measured toner usage of each page in a set of training pages, and the histogram of the pixel values for the predicted scanned pages in the training set. Compared with the pixel counting method and our previous two-stage predictor, the updated approach is not only more robust and accurate, but also more suitable for hardware design.

***Keywords*—absorptance prediction, toner usage estimation, laser electrophotographic printer.**

I. Introduction

The cost of consumables, specifically toner cartridges, has always been an area of concern for customers. The issue becomes especially acute when the price of a complete set of replacement cartridges approaches the cost of the new printer itself. With the growing popularity of managed print services, accurate control of the cost of consumables takes on an entirely new urgency for the vendor.

When using a printer, it is undesirable that poor print quality due to toner depletion or unexpected low levels of cartridges caused by inaccurate prediction of toner rated life occurs during a series of print jobs. For customers who do not have a replacement on hand, this problem is especially important. Additionally, when a printer outputs faded pages before the cartridge reaches the end of life that the customer expect. He or she tends to assume that they incurred unnecessarily high cost for their cartridges. For improving the printing experience for customers, a more accurate end-of-life prediction is necessary to be implemented for cartridges, which will anticipate and prevent the above situations. Therefore, an accurate toner usage predictor is needed.

During the laser electrophotographic printing process, the prediction of toner usage is not only influenced by a single given printer-addressed pixel value, but also by the neighboring pixels within an area. The interaction between neighboring pixels is nonlinear and complex, which is the biggest challenge of toner usage estimation. The size of a single pixel is smaller than the spot size of a laser beam; therefore an overlap between laser spot and individual pixels occurs. The process of toner transferring from the developer roller to the organic photoconductor drum, then to the intermediate transfer belt, then to the media and finally to be fused to the media all cause further toner spreading.

The accurate estimation of toner usage for laser electrophotographic printing should not only consider the pixel-by-pixel gray level in the digital image that needs to be printed, but also take the spatial distribution of the neighboring pixels for each pixel in the digital image into account. While current pixel-counting approaches attempt to account for this in a limited way, these methods are too simplistic to yield the level of desired accuracy. For instance, U. S. Pat. No. 5,349,377 [1] estimates the consumption of toner by analyzing the frequency rate of 1s and 0s in the halftone image, and calculates the weighting factors for different types of images. U. S. Pat. No. 7,720,397 [2] introduces a method that accounts for the diffusion effect caused by non-adjacent pixel groups. The system determines a proximity factor that is indicative of the number of independent pixel groups within each set of eight adjacent pixels, and then computes toner usage based on the proximity factor and pixel count for the page. The two approaches listed above are not sufficiently comprehensive to account for the complicated interaction between pixels.

Our updated two-stage method[1] is developed based on the traditional two-stage approach studied by Wang [3] and the 'black box' model investigated by Ju [4]. The first stage of the updated method is to predict the pixel-by-pixel based absorptance for all pixels in the digital input. During the second stage, a weight will be assigned to each pixel based on the absorptance value. Ultimately, the toner usage for the entire input page can be predicted by accumulating the weights for all pixels.

II. Our Approach

In the EP process, each of the C, M, Y and K channels is treated separately. This paper mainly describes the implementation of the K channel. However, our algorithm

[1]Research supported by the Hewlett-Packard Company, Palo Alto, CA.

should be broadly applicable to all four color channels.

A. Stage one: absorptance predictor

1) Training pages design

There are five training pages for stage one, which include two text pages with different font sizes, one page with horizontal and vertical lines and two 256 level monochrome continuous-tone images. Figure. 1 displays each of the stage one training pages. Each training page is quantized to 32 levels.

Figure. 1: Stage one training pages.

The random text training pages (1 and 2) consisting of meaningless words as shown in Figure. 1 are generated using the software, "Monkey Random Text Generator" [7]. All letters are chosen from the 52 letters of the alphabet including all small and capital letters from "a" to "z" and "A" to "Z", and are written in Times New Roman typeface with 12 point size. The Mixed line file (training page 3) has horizontal and vertical lines with different line widths (1 pixel to 10 pixels). For each of the training pages, fiducial marks are printed every 265 printer pixels for alignment that helps to locate each pixel of interest. As shown in Figure. 2, the size of a fiducial mark is 5×5 pixels and surrounded by 25×25 pixels white space, which is a safe distance to ensure that the fiducial marks do not influence the printed absorptance of the page content. Inside of the 265×265 pixels fiducial-mark block, there is a 200×200 pixels analysis area, where the printed absorptance of every pixel in the analysis area will contribute to the training data. Absorptance value ranges from 0 to 255, where 0 represents white and 255 represents black. In each training page, there are 20 rows and 15 columns of analysis areas, which means that there exist $200 \times 200 \times 15 \times 20 = 12,000,000$ pixels to be analyzed.

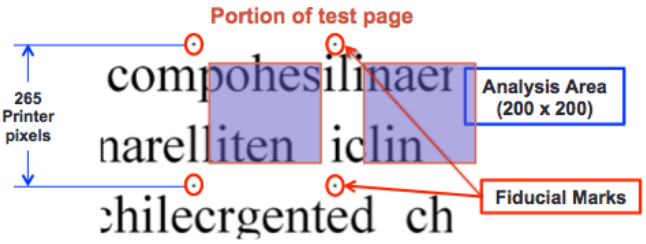

Figure. 2: A cropped portion of the text file.

2) Absorptance estimation

The designed test pages (with fiducial marks) are then printed at 600 dpi by a target laser electrophotographic printer at 600 dpi; then scanned at 1800 dpi by an Epson 10000XL scanner. The actual scanned pages are calibrated using the method of scanner gray balancing [8] in order to be consistent with the appearance of the printed page. After calibration, the gray values of scanned pages will be proportional to 1 minus CIE Y (luminance) value scaled to lie between 0 and 1, and will vary from 0 to 1. The size of a printer-addressable pixel is $\frac{1}{600}$ inch because the training page is printed at 600 dpi; and the size of a scanner-addressable pixel is $\frac{1}{1800}$ inch since the scanner resolution is chosen to be 1800 dpi. Therefore, every printer pixel corresponds to 3×3 scanner pixels; thereby the absorptance of printed pages can be estimated through the scanned pages.

Then, the center coordinates (centroid) of each fiducial mark will be determined. The centroid of each fiducial mark is calculated based on the spatial distribution of toner absorptance throughout its corresponding mask region. First, the horizontal and vertical centroids of the i^{th} segmented fiducial mark are calculated by

$$C_{x,i} = \frac{\sum_{[k,l]\in D_i}(k-0.5)s[k,l]}{\sum_{[k,l]\in D_i} s[k,l]}, \quad (1)$$

and

$$C_{y,i} = \frac{\sum_{[k,l]\in D_i}(l-0.5)s[k,l]}{\sum_{[k,l]\in D_i} s[k,l]}, \quad (2)$$

where D_i is the corresponding binary mask for the i^{th} fiducial mark in the binary mask image. The binary mask image is generated using the Otsu's method. The parameter $s[k,l]$ is the absorptance value of the scanned image at the pixel with coordinates $[k,l]$. The 0.5-pixel offset in both Eqs. (1) and (2) shifts the effective coordinate location of each pixel to its center.

3) Assigning dot configuration values (encoding)

Next, the coordinates for all printer pixels of interest in the 200×200 analysis area will be determined based on the centroids of the fiducial marks. The absorptance of each analyzed printer pixel is measured by averaging the absorptance in the

corresponding 3×3 scanner-pixel area. An index ranging from 1 to 25 is assigned to each pixel in the 5×5 predictor window, the 17 contributing pixels that are shown in Figure. 3 have indices $[1,3,5,7,8,9,11,12,13,14,15,17,18,19,21,23,25]$. Since the absorptance of a pixel is influenced by its surrounding pixels, we consider a 5×5 window:

- A dot configuration value will be assigned to the center pixel in the 5×5 window based on the pixel values of all 17 contributing pixels and their positions in the window. Each such pixel is an integer between 0 and 31 that can be represented by 5 bits.
- Every pixel of interest in the input image will have a dot configuration value that is represented by five numbers, as described below.

As shown in Figure. 3, the center pixel is pixel No. 9. The dot configuration value of the center pixel is formed by five numbers a, b, c, d, and e that can be determined by the following equations:

$$\begin{aligned}
a &= 2^{10}\times p(1)+2^{5}\times p(2)+2^{0}\times p(3),\\
b &= 2^{10}\times p(4)+2^{5}\times p(5)+2^{0}\times p(6),\\
c &= 2^{20}\times p(7)+2^{15}\times p(8)+2^{10}\times p(9)\\
&\quad +2^{5}\times p(10)+2^{0}\times p(11),\\
d &= 2^{10}\times p(12)+2^{5}\times p(13)+2^{0}\times p(14),\\
e &= 2^{10}\times p(15)+2^{5}\times p(16)+2^{0}\times p(17),
\end{aligned}$$

where p(i) is the pixel value of the i^{th} (i = 1,...,17) pixel in the window.

After assigning the dot configurations to all pixels of interest, a table that contains the coordinates of the pixel, the corresponding estimated absorptance, and the dot configuration values will be built. Some of the dot configuration values will be the same, the value is stored only once, and the average estimated absorptance for the pixels that have the same dot configuration values is recorded. The information of the diplicate dot configuration values will be removed. The stored dot configuration values are called the unique dot configurations.

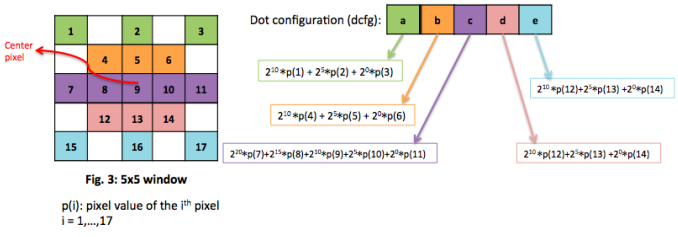

Figure. 3: Assigning a dot configuration value to the center pixel in the 5×5 window of interest.

4) Obtaining pixel values from unique dot configuration values (decoding)

The following method will be used to obtain the pixel values of each of the 17 pixels by using the five numbers that comprise a single dot configuration value. For example, in Figure. 3, the pixel values of pixel No. 1, 2, and 3 will be calculated based on the first value (a) of the dot configuration.

$$\begin{aligned}
\frac{a}{32} &= \frac{2^{10}\times p(1)+2^{5}\times p(2)+2^{0}\times p(3)}{32}\\
&= \underbrace{2^{5}\times p(1)+2^{0}\times p(2)}_{\text{quotient}}+\underbrace{p(3)}_{\text{remainder}}.
\end{aligned}$$

The remainder is the value of pixel No. 3.

Now, divide the quotient by 32, the remainder will be the value of pixel No. 2.

$$\frac{2^{5}\times p(1)+2^{0}\times p(2)}{32} = \underbrace{2^{0}\times p(1)}_{\text{quotient}}+\underbrace{p(2)}_{\text{remainder}}.$$

Again, divide the quotient by 32, and the remainder will be the value of pixel No.1. This method is repeated until the values of all pixels of interest in the digital input are calculated.

Then, a vector with size of 32 will be created to store the pixel values. If the pixel value is $p(i)$ ($p(i)$ = 0,...,31), a '1' is assigned to the $(p(i)+1)^{\text{th}}$ element of the vector. For instance, if the value of pixel No. 1 is 0, the vector will be:

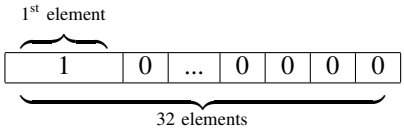

Considering all 17 pixels in the 5×5 window, there will be a long vector with size of 32×17 storing the pixel values of 17 pixels, where the first 32 elements represent pixel No.1, and the last 32 elements represent pixel No.17. Since one dot configuration can decode 17 pixel values, then if there are n unique dot configurations, there will be a matrix as shown in Table. I with size of $n\times(32\times17)$, where n is the number of rows and (32×17) is the number of columns.

TABLE I: Example of matrix that stores the pixel values of all pixels of interest

	1	2	...	32×17
1	1	0	...	0
2	0	...	1	0
⋮	0	...	...	1
$n-1$	0	0	...	0
n	0	...	1	0

The absorptance predictor, which is also called a Look-up table (LUT), is optimized by the least squares regression algorithm [5],[6] based on the pixel values and positions of

the 17 contributing pixels that are decoded by the unique dot configuration and the relative average estimated absorptance.

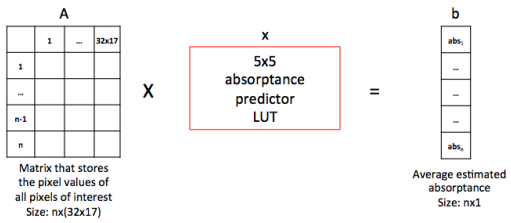

Figure. 4: Stage one LUT optimization.

5) Generating the stage one look-up table by using least squares method

In Figure. 4, assume matrix A is the matrix that stores the pixel values, vector b is the matrix that contains the average estimated absorptance, and the unknown x is the stage one LUT that needs to be solved. The size of b is $n \times 1$, because there are n unique dot configurations. The equation is simplified to be $Ax = b$. Then by using the least squares method, the unknown x can be determined by:

$$x = (A^T A)^{-1} A^T b$$

The LUT has 32 rows that represent 32 different pixel values, and 17 columns stand for 17 different positions for contributing pixels. For instance, in Figure. 5, pixel No. 1 is the first contributing pixel, and pixel No. 25 is the last contributing pixel; thereby, pixel No. 1 takes the first pixel position and pixel No. 25 is in position 17. The absorptance predictor will be used to predict the absorptance of the center pixel in each 5×5 neighborhood.

6) Absorptance prediction

Since the absorptance of a certain printed pixel is influenced by the distribution of its 5×5 surrounding pixels in the digital image, the absorptance predictor is proposed as in Figure. 5. If all the pixels within the 5×5 window have the same value for 32 level digital images, the average absorptance at the same pixel value will be use to predict the absorptance of the center pixel. The average absorptance is determined by averaging the estimated absorptance of the center pixels whose 5×5 surrounding pixels are constant. Otherwise, the absorptance predictor LUT will be applied to predictor the absorptance.

B. Stage two: toner usage predictor.

The toner usage prediction is a mapping from the absorptance predictions to a toner usage prediction. The mapping is built based on 45 training pages, which contain 1-pixel-wide to 10-pixel-wide horizontal and vertical lines pages, random text with different typefaces, point sizes, and line spacings, and 8-bit per pixel digital pages with different type of contents (text, figures, and images).

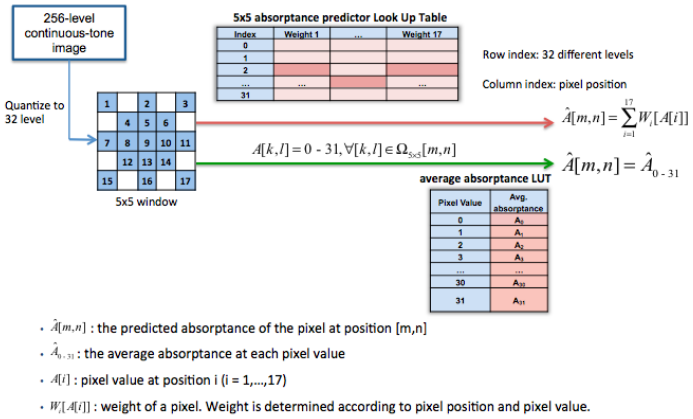

Figure. 5: Structure of the absorptance predictor.

The actual toner usage is measured by printing 100 copies of each test page to reduce the experimental error. The measurement is implemented by splitting and weighting the black cartridge before and after the 100-copy printing job. Let's denote the toner usage per single page as $m_{toner,i}$, $i = 1, ..., 45$.

To obtain the toner usage mapping, first the pixel-by-pixel absorptance of the 45 test pages is predicted by using the absorptance predictor. Then, the histograms of these predicted scanned pages are calculated. The predicted absorptance is expected to be related to the toner mass. Assuming that the mapping can be constant within reasonably divided absorptance ranges, the Lloyd-Max Algorithm is applied to the histograms to obtain the absorptance bins and accumulate the number of pixels that fall into each bin. Finally, the least squares regression method [5],[6] is used to determine the toner usage mapping table $[w_{range1}, ..., w_{rangeM}]^T$ based on the selected bins and the histograms as shown in Eq. (3). The toner usage mapping table is shown in Table II.

$$\begin{bmatrix} h^1_{range1} & \cdots & h^1_{rangeM} \\ \vdots & \ddots & \vdots \\ h^{45}_{range1} & \cdots & h^{45}_{rangeM} \end{bmatrix} \begin{bmatrix} \overset{i}{w_{range1}} \\ \vdots \\ w_{rangeM} \end{bmatrix} = \begin{bmatrix} \overset{j}{m_{toner1}} \\ \vdots \\ m_{toner45} \end{bmatrix} \quad (3)$$

Here M is the number of bins, and h^j_{rangei} is the number of pixels that fall in the i-th bin of the j-th training page.

III. Implementation of the Two-Stage Approach

Considering the entire system, Stage one uses the absorptance look up table to predict the absorptance of the input 256 level digital monochrome image, and Stage two accumulates the weight of each pixel based on the weight mapping table to get the toner usage for the whole page. Figure. 6 describes the overall algorithm of the updated two-stage method.

TABLE II: Absortptance ranges and the corresponding toner usage weights

Range index	Range	Weight	Range index	Range	Weight
1	$[1, 7)$	0.0784	17	$[129, 136)$	0
2	$[7, 16)$	0.0238	18	$[136, 145)$	0
3	$[16, 25)$	0.0147	19	$[145, 153)$	0
4	$[25, 32)$	0.047	20	$[153, 160)$	0
5	$[32, 39)$	0.0584	21	$[160, 169)$	0.1659
6	$[39, 48)$	0.0004	22	$[169, 178)$	0.0022
7	$[48, 57)$	0.1945	23	$[178, 185)$	0.1914
8	$[57, 63)$	0.0684	24	$[185, 194)$	0.0345
9	$[63, 73)$	0	25	$[194, 201)$	0
10	$[73, 81)$	0	26	$[201, 210)$	0
11	$[81, 88)$	0.1275	27	$[210, 218)$	0.0709
12	$[88, 96)$	0.1221	28	$[218, 225)$	0.0953
13	$[96, 105)$	0	29	$[225, 233)$	0.3334
14	$[105, 114)$	0.3652	30	$[233, 242)$	0
15	$[114, 122)$	0.4562	31	$[242, 251)$	0.1288
16	$[122, 129)$	0	32	$[251, 256)$	0.0938

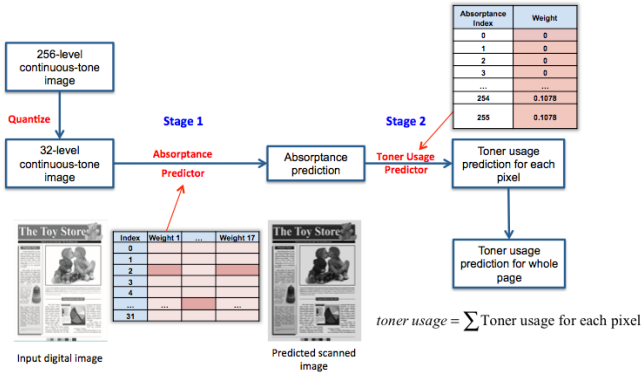

Figure. 6: Implementation of toner usage predictor.

IV. Experimental Result

Five-fold cross validation was performed to evaluate the accuracy of the two-stage predictor. The 45 Stage two training pages were divided into five groups with each group containing nine representative pages. Each one of the groups is used as a training set while the remaining four groups are testing sets. The grouping procedure is randomized 25 times in order to obtain more realistic results by taking the average of the total 125 trials. Figure. 7 shows the average absolute relative error for each of the 45 training pages. Table III displays the mean absolute relative error, the standard deviation, the maximum and minimum absolute relative error across 45 pages.

TABLE III: Average prediction errors across 45 test pages

Mean absolute relative error (%)	2.23
Mean standard deviation (%)	1.20
Maximum relative error (%)	2.79
Minimum relative error (%)	0.36

The updated two-stage approach reduces the size of absorptance LUT and uses a more stable quantizer to build the

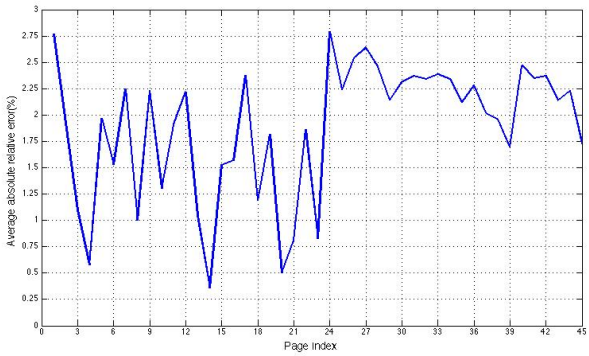

Figure. 7: Prediction error of each test page.

weight mapping table. Comparing the cross validation result with that of our previous predictor [3], the standard deviation of the mean absolute relative error for the updated two-stage algorithm is 1.20%. However, the result for our previous work is approximately 5 times larger, which proves that the current algorithm provides a more stable result. Furthermore, the updated two-stage algorithm is confirmed to be hardware implementable because of the size reduction for the absorptance LUT.

V. Conclusion

The ability to accurately estimate toner consumption plays into numerous financial aspects of products. It is of great importance not only for the printer/cartridge manufacturer, but also for the customer who wants to fully utilize every cartridge while providing great printed output.

Our two-stage toner usage predictor is for electrophotographic laser printers. The predictor consists of an absorptance predictor that determines the absorptance from printed and scanned pages, and a toner usage map, which converts the absorptance into toner usage. The predictor is on 45 arbitrarily chosen test pages by using five-fold cross validation. Our two-stage predictor yields a much more accurate prediction of toner consumption and more consistent predictions. also, very importantly, this two-stage predictor is more suitable for hardware implementation than our previous predictor [3].

REFERENCES

[1] Gilliland, W. K., Midgley, C. G., Murphy, A. M., and Bowerman, W. T.,"Printer Toner Usage Indicator with Image Weighted Calculation," *U.S. Pat. 5,349,377* (1994).

[2] Filbrich, W., and Brent R., "Systems and methods for monitoring toner usage," *U.S. Pat. 7,720,397* (2010).

[3] Wang, L., Abramsohn, D., Ives, T., Shaw, M.Q., and Allebach, J.P., "Estimating toner usage with laser electrophotographic printers," in *Color Imaging XVII: Displaying, Processing, Hardcopy, and Applications,* SPIE Vol. 8652 (2013).

[4] Ju, Y., Kashti, T., Frank, T., Kella, D., Shaked, D., Fischer, M., Allebach, J.P., "Black-Box Models for Laser Electrophotographic Printers–Recent Progress," in *NIP and Digital Fabrication Conference,* IS&T Vol. 2013 (2013).

[5] Barrett, R., Berry, M. W., Chan, T. F., Demmel, J., Donato, J., Dongarra, J., and Van der Vorst, H., *Templates for the solution of linear systems: building blocks for iterative methods,* SIAM Vol. 43 (1994).

[6] Paige, C. C., and Saunders, M. A., "LSQR: An algorithm for sparse linear equations and sparse least squares," *ACM Transactions on Mathematical Software,* TOMS Vol. 8 (1982).

[7] Mikkilineni, A. K., Ali, G. N., Chiang, P. J., Chiu, G. T., Allebach, J. P., and Delp, E. J., "Signature-embedding in printed documents for security and forensic application," in *security, Steganography, and Watermarking of Multimedia Contents VI* SPIE Vol. 5306 (2004).

[8] Gindi, S. A., "Color Characterization and Modeling of a Scanner," *M.S. Thesis* Purdue University (2008).

[9] Hastie, T., Tibshirani, R., Friedman, J., and Franklin, J., "The elements of statistical learning: data mining, inference and prediction," *The Mathematical Intelligencer* (2005).

AUTHOR BIOGRAPHIES

Mengqi Gao received her B.S. in Electrical Engineering from Purdue University (2014) and is currently studying for the M.S. in Electrical Engineering. Her primary area of research has been image processing, image segmentation and image quality evaluation.

Yanling Ju received her B.S. degree in electrical engineering from Peking University, Beijing, China, in 2006 and M.E. degree from the Graduate School of Chinese Academy of Science, China, in 2009. In 2015 she received her Ph.D. degree from the School of Electrical and Computer Engineering, Purdue University, West Lafayette, IN. She currently works for Medica, Boston as an image processing and pattern recognition software engineer. Her research interests are focused on image processing, image quality evaluation, computer vision and pattern recognition.

Terry Nelson has been a Development Engineer with Hewlett Packard for over 35 years. He started sparking with a Tesla Coil, radios, and HP calculators. After reviving an AAS in electronics from Spokane Community College in 1979, he joined Hewlett-Packard Company working disk storage technology. Moving to printing, he developed systems for ink jet, wet/dry electro-photography, and machine control. Several years were spent doing system modeling, image processing, color science, system testing, and way too many programming languages. Along the way he picked up eight patents in ink jet, image processing, data compression, color science, and printer calibration

Theresa Prenn received her B.S.E.E. degree from The University of Michigan in 1990. She has worked for Hewlett-Packard for the past 25 years. She has been actively involved in designing ASICs for the last 21 years for the LaserJet R&D Lab. Her five patents to date involve printing architecture and image data processing algorithms. Her work can be found across the entire portfolio of mono and color LaserJet printers. Prior to HP, Theresa worked at Lionel Trains Inc. designing and building test equipment.

Jan P. Allebach is Hewlett-Packard Distinguished Professor of Electrical and Computer Engineering at Purdue University. Allebach is a Fellow of the IEEE, the National Academy of Inventors, the Society for Imaging Science and Technology (IST), and SPIE. He was named Electronic Imaging Scientist of the Year by IS&T and SPIE, and was named Honorary Member of IST, the highest award that IST bestows. He has received the IEEE Daniel E. Noble Award, and is a member of the National Academy of Engineering. He currently serves as an IEEE Signal Processing Society Distinguished Lecturer (2016-2017).